Available online at www.sciencedirect.com

ScienceDirect

Mendeleev Commun., 2022, **32**, 510–513

Mendeleev Communications

Effect of textural characteristics on the catalytic performance of supported $KCoMoS_2$ in the synthesis of higher alcohols from syngas

Mohamed E. Osman,*[a,b] Vladimir V. Maximov,[a] Tshepo D. Dipheko,[a,b] Tatiana F. Sheshko,[b] Alexander G. Cherednichenko[b] and Victor M. Kogan[a]

[a] *N. D. Zelinsky Institute of Organic Chemistry, Russian Academy of Sciences, 119991 Moscow, Russian Federation. E-mail: wadalmsna3.com@gmail.com*

[b] *Peoples Friendship University of Russia (RUDN University), 117198 Moscow, Russian Federation*

DOI: 10.1016/j.mencom.2022.07.026

The influence of textural characteristics on the catalytic performance of supported $KCoMoS_2$ catalysts was explored to provide essential information for the design of better catalysts for the synthesis of higher alcohols (C_1–C_5) from syngas. Syngas conversion was carried out over $KCoMoS_2$ catalysts supported on various mesoporous (alumina and carbon-coated alumina) and microporous (two types of powdered activated carbons) materials. The experimental results show that catalysts supported over microporous materials exhibit higher catalytic activity in HAS from syngas than catalysts based on mesoporous materials.

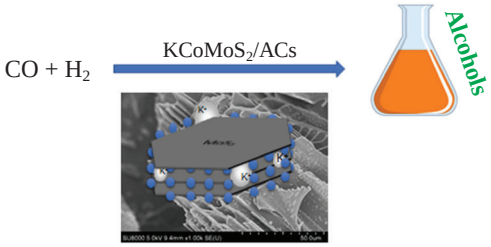

Keywords: syngas, alcohols, alkanols, heterogeneous catalysis, transition metal sulfide catalysts, cobalt compounds.

Several catalytic systems for the higher alcohols synthesis (HAS) from syngas are known, among which the most promising are those based on MoS_2 promoted by cobalt or nickel and modified with alkali metals.[1–5] Syngas conversion on unpromoted MoS_2 yields mainly hydrocarbons, whereas MoS_2 modified with potassium and heavier alkali metals gives mainly alcohols. The second transition metal deactivates the sulfur-edge but promotes activity of the M-edge resulting in increased selectivity towards alcohols.[6] Modification with alkali metals causes a decrease in the number of MoS_2 slabs, which in turn leads to an increase in the catalyst affinity for sulfur and a decrease in Lewis acidity, preventing hydrogenation and hydrodeoxygenation.[7]

The most important properties of active carbons (AC) as catalyst supports compared to oxide supports (Al_2O_3, SiO_2, TiO_4, *etc*.) are facile recovery of the active metal by combustion of the carbon support, neutral nature (no strong acidic or basic sites), and cost efficiency.[8,9] Several studies examined the effect of textural characteristics of supports on the active phase of K-modified CoMoS and on the catalytic performance in HAS. Some of these studies experimented with mesoporous materials such as metal oxides[10] and multi-walled carbon nanotubes (MWCNT),[11] while others utilized microporous activated carbons.[12,13]

In this work, the effect of textural characteristics of supports and supported $KCoMoS_2$ catalysts on the catalytic performance in HAS was studied using two types of mesoporous materials (Al_2O_3 and carbon-coated alumina, CCA) and two types of microporous powdered activated carbons, BAW and AG-3, obtained from birch and coal semi-coke, respectively. Experimental details are described in Online Supplementary Materials, where the textural characteristics of the supports and the supported $KCoMoS_2$ catalysts are summarized in Table S2. Loading of the support material with the active phase reduces both the specific surface area and the pore volume [Figure S1(*a*),(*b*)]. The ratio between micro- and mesopores of the tested catalysts is clearly seen from Figure S1(*c*),(*d*) showing the surface area and the pore volume of micro- and mesopores, respectively.

According to the textural characteristics of the carriers and catalysts supported on corresponding carriers (see Figure S1), S_{total} of the supports decreases in a sequence: CCA < Al_2O_3 < < BAW < AG-3. Value V_{total} tends to decrease in a sequence: Al_2O_3 > CCA > AG-3 > BAW. The difference in the order is due to the difference in the pore composition: AG-3 and BAW contain much more micropores (pore volume ⩽ 4 nm) than Al_2O_3 and CCA. Specifically, alumina does not contain micropores at all and the specific surface area of micropores of the rest materials decreases in a sequence: AG-3 > BAW > CCA > > Al_2O_3. Supports Al_2O_3 and CCA contain only macro- and mesopores, whereas AG-3 and BAW consist mainly of microporous structures.

Scanning electron microscopy (SEM) images of the supports and the supported catalysts are shown in Figures S2–S5. The image of the alumina support shows multiple fine particles with some larger agglomerates. During coating with carbon, the surface is smoothed out, and larger features become more visible. In both cases, the surface of the prepared catalyst is dominated by a smooth gel-like phase with dotted fine particles and a few large nano crystal agglomerates. The observed particles are significantly larger than those in the original alumina. The AG-3 sample consists of numerous small platelets dotted with small holes. The platelets form fairly large agglomerates with pores between them. The platelets in the prepared catalyst are not visible, the surface is smooth, and no crystalline particles are

visible. Only larger pores are observed. The BAW support inherited from the parent timber rather large cylindrical pores with relatively smooth walls. The cylinder walls are dotted with small holes. Macropores are embedded in a microporous matrix with an irregular cross-section. During the catalyst preparation, the rough cross-section is replaced by the smooth surface and the walls of the large channel become uneven.

In all cases, crystallites of the active phase are small (normally below 5 nm) and can be observed only at high magnification.[14] Therefore, the crystallites were analyzed by transmission electron microscopy (TEM, see Online Supplementary Materials, Figure S6). In Figure S6, molybdenum disulfide slabs are readily visible as threadlike fringes in the multilayer particles of the active phase of $KCoMoS_2$ with varying degrees of stacking. The significant differences between the samples are due to the interaction between the active phase and the supports.[14] Catalyst CCA shows the increase in stacking compared to bare Al_2O_3. The number of stacked crystallites on BAW is greater than that on AG-3. In the active phase, a higher stacking degree causes the increase in basal and corner sites, which leads to the decrease in hydride hydrogen adsorption.[15,16]

Data on acidity of the supports and catalysts are given in Figure S7. Acidity of the supports and catalysts increased in a sequence: BAW < AG-3 < CCA < Al_2O_3. The carbon-supported sulfided catalysts showed higher acidity than the bare support materials. Acidity decreased upon addition of the active phase only in the case of pure alumina. Presumably, the active phase of $KCoMoS_2$ has its own acidity which is much lower than that of alumina but higher than that of the other C-containing materials. Figure S7 shows that acidity is detrimental for CO conversion: the catalyst with higher acidity (Cat-Al_2O_3) gave lower CO conversion (30.3%), whereas the catalyst that exhibited lower acidity (Cat-BAW) had higher CO conversion (43%). Carbon on CCA decreased acidity of Al_2O_3 (see Figure S7), which promoted CO conversion.

Microporous catalysts were found to be more active with respect to CO conversion than mesoporous catalysts. Figure S8 shows a relation between CO conversion and the total meso- and micropore specific surface area and volume. The dependence of CO conversion on V_{meso} grows significantly faster than on S_{meso} in the interval from Cat-Al_2O_3 to Cat-CCA. The changes in CO conversion as a function of the surface area and volume of micro- and mesopores look similar in plots (*a*) and (*b*) in Figure S8. The observed difference can be explained by amorphous carbon present on the alumina surface of the CCA support as described earlier.[15] If we assume a simplified cylinder model for a mesopore [Figure S9(*a*)] with the amorphous carbon coating on its internal surface [Figure S9(*b*)], we can see that the decrease in the pore volume will be less significant than reduction of the internal surface [Figure S9(*c*)].

Since CO conversion *versus* the mesopore specific surface increases more than *versus* the mesopore volume for Cat-CCA compared to Cat-Al_2O_3, carbon cannot fill the entire volume of Cat-CCA mesopores, as shown in Figure S9(*d*). Coating the mesopore walls with a monolayer (less probable case) or islands (more probable case) of amorphous carbon causes a decrease in the number of alumina hydroxyl groups in the CCA carrier and, thus, to a decrease in the interaction between the active phase and support material, which leads to enhanced catalyst activity in CO conversion.

Selectivity for CH_4 was found to be higher than that for C_2–C_4 hydrocarbons for all catalysts. Furthermore, a positive correlation was noted between methane selectivity and the micropore surface area and volume (see textural results in Table S2). Ethanol was the main product for all supported $KCoMoS_2$ catalysts (Figure 1).

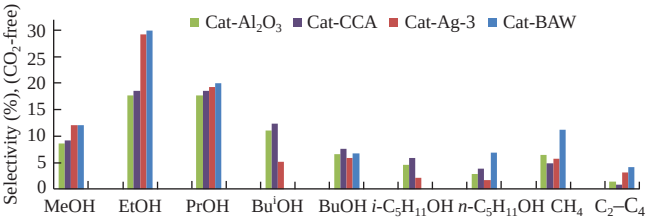

Figure 1 Selectivity for different alcohols, CH_4, and C_2–C_4 hydrocarbons over supported $KCoMoS_2$ catalysts. Reaction conditions: T = 360 °C, P = 5.0 MPa, $CO/H_2/Ar$ = 45 : 45 : 10, GHSV = 460 h^{-1}, catalyst loading 3 g.

Selectivity towards methanol, ethanol, and *n*-propanol decreased in a sequence: Cat-BAW > Cat-AG-3 > Cat-CCA > > Cat-Al_2O_3. $KCoMoS_2$/BAW did not produce any isobutanol or isopentanol, whereas the Cat-CCA supported catalyst gave the highest yield of isopentanol alcohol. The highest selectivity for CH_4 and C_2–C_4 hydrocarbons was observed at 360 °C. Methane selectivity depends on the nature of the catalyst support and increases in the following sequence: Cat-CCA < Cat-Al_2O_3 < < Cat-AG-3 < Cat-BAW (see Figure 1). Additionally, selectivity including CO_2 is represented in Table S3 (see Online supplementary Materials). The CO_2 selectivity tends to be decreased in a sequence: Cat-Al_2O_3 > Cat-CCA > Cat-AG-3 > > Cat-BAW. The best results of ACs supported catalysts can be attributed to the properties of ACs (mentioned above) that make the catalysts capable to resist the water–gas shift reaction. The CO_2 selectivity shows a positive correlation with the catalysts acidity.

Figure 2 depicts the ratio between alcohol and hydrocarbon yields ($Y_{ROH/HCs}$) for the catalysts; it increases as follows: Cat-AG-3 < Cat-Al_2O_3 < Cat-CCA < Cat-BAW. The highest $Y_{ROH/HCs}$ for Cat-BAW can be attributed to its largest total and micropore surface area, as well as to the micropore volume [Table S2 and Figure S1(*a*)]. In general, a large surface area (500 m^2 g^{-1} for BAW) increases catalytic performance of AC supported catalysts, as well as their stability in basic or acidic media and towards severe reaction conditions such as high pressure and temperature. In the case of the supported $KCoMoS_2$ catalyst, a minimal active phase–support interaction is also beneficial.[17] The value $Y_{ROH/HCs}$ increased when alumina was coated with carbon due to a lower active phase–support interaction. All previously discussed results relate to the textural characteristics of the catalysts, particularly S_{micro}, V_{micro}, S_{meso}, and V_{meso}.

The yield of alcohols also correlates with the micropore surface and volume (Figure S10). The plateau achieved by the alcohol yield in correlation with the micropore structure of Cat-AG-3 and Cat-BAW corresponds to the optimal micropore size. In contrast, catalytic activity dependences on the specific surface area of mesopores (S_{meso}) and the pore volume (V_{meso}) demonstrate the opposite trend: fewer mesopores lead to higher catalytic activity (Figure S11).

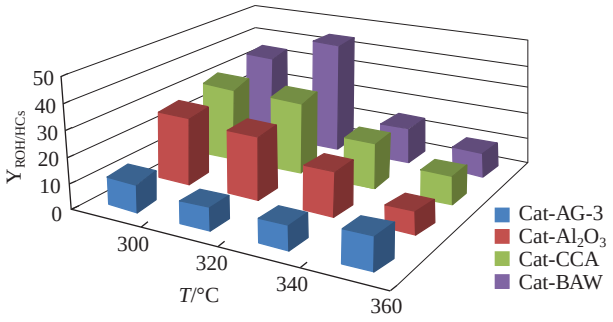

Figure 2 Ratio of alcohol/hydrocarbon yields ($Y_{ROH/HCs}$) at various temperatures. For reaction conditions, see Figure 1.

Figure 3 shows that ethanol, propanol and methanol are the main alcohol products for the tested catalysts. Their yield increases with the increasing surface and volume of micropores and decreases with the increasing surface and volume of mesopores. The yield of *n*-butanol is not related to porosity of the carrier. *n*-Pentanol is a minor product. Isobutanol and isopentanol contents display opposite trends compared to the main products, decreasing with the increasing micropore surface and volume and increasing with the increasing mesopore surface and volume. Microporous carriers inhibit isomerization due to steric constraints. The lowest selectivity toward isoalkanols over Cat-BAW is attributed to the low acidity of the catalyst because the acid sites catalyze the isomerization reactions.[18] Figure 3 also shows that the highest yields of methanol, ethanol, propan-1-ol, isobutanol, pentanol and isopentanol were achieved at 360 °C for all catalysts. Propan-2-ol and butan-2-ol appeared only over Cat-CCA. Linear alcohol yields decreased in the following sequence: Cat-BAW > Cat-AG-3 > Cat-CCA > CatAl_2O_3; isoalkanol yields decreased in the reverse sequence: CatAl_2O_3 > Cat-CCA > Cat-AG-3 > Cat-BAW.

The results disagree with the statement[12] where the authors found that the mesoporous MWCNT-supported K-modified trimetallic C–Rh–Mo catalyst exhibited higher catalytic activity in HAS from synthesis gas than microporous activated carbon-supported catalysts of the same composition. They believed that CO conversion and alcohol yields were not related to the surface area and pore volume of the support, whereas the textural properties of the support such as pore size and mesoporosity had a direct influence on the synthesis of mixed alcohols from synthesis gas. At the same time, they argued that dispersion of mesoporous MWCNT-supported catalysts was lower than that of microporous activated carbon-supported ones. This is consistent with our results on the formation of giant CoMoS agglomerates on mesoporous alumina and CCA (see Figures S4 and S5). As follows from their results, even a small number of mesopores is better than a large number of micropores. Comparing their materials with ours, one can see that the two catalysts showing better results in syngas conversion, such as AG-3 and BAW supported catalysts, contain both meso- and micropores in the carrier with a vast majority of micropores, whereas the alumina and CCA-based catalysts contain almost only mesopores in the carrier (see Figure 1). In addition, BAW contains large channels with a great number of meso- and micropores in their walls of complex structure (Figure S5). We believe that the contradiction can be resolved if to assume that the presence of different functional groups on the carbon surface is a crucial factor that

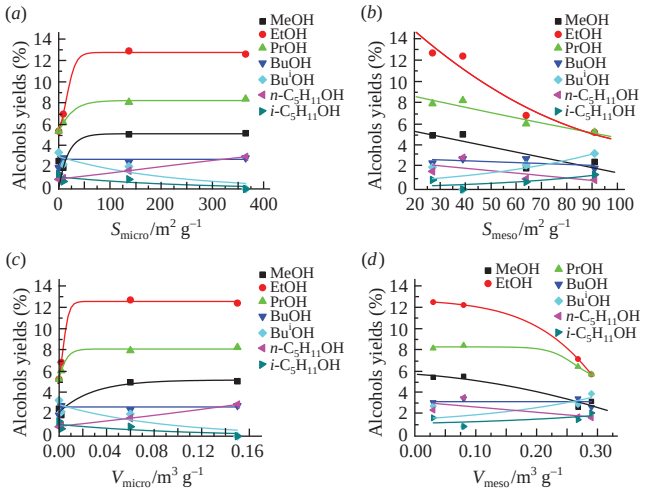

Figure 3 Dependences of specified alcohol yields on parameters (*a*) S_{micro}, (*b*) S_{meso}, (*c*) V_{micro} and (*d*) V_{meso} at 360 °C.

reduces catalytic activity and alcohol selectivity of carbon-supported materials. Such functional groups may strongly interact with the active phase and increase acidity of the carrier. Both factors negatively affect catalytic activity.[16] Thus, we suppose that the MWCNT material used in previous study[12] contained fewer functional groups than activated carbon-based materials. It would be interesting to consider the contribution of each product to the total alcohol yield depending on the pore structure. Acidity of the catalysts also supports this interpretation. The discrepancy between the results obtained in reported study[12] and our findings may also be attributed to the use of citric acid during one-step wetness impregnation in our case. During sulfidation, citric acid and citrates decompose to give amorphous carbon. This carbon fills micropores, which prevents the penetration of the active phase into micropores, reducing dispersion and leading to the formation of large smooth crystallites with a higher number of facets, which is favorable for HAS.

The data outlined in Figure S12 (see Online Supplementary Materials) were obtained from HRTEM statistics. The ACs supported catalysts are characterized by a higher stacking number and average slab length compared to the alumina and CCA samples. These results are attributed to the active phase interaction with the support being weakened, and also forming of MoS_2 crystallites out of pores. The relative content of mono- and bi-layered crystallites of Cat-AG-3 and Cat-BAW were found to be almost half of Cat-Al_2O_3 and Cat-CCA. On the other hand, the content of 3, 4, 5, 6, and 7 stacked slabs of BAW and AG-3 were found to be higher compared with the counterparts. Only the Cat-BAW shows high content of 8-stacked slabs. The highest content has been observed for particle length between 4-6 nm in all catalysts except in Cat-BAW, the highest content has been determined for particles which are longer than 10 nm. The results in Figure S13 corroborate the catalytic performance of our catalysts (Cat-Al_2O_3 < Cat-CCA < Cat-AG-3 < Cat-BAW). The higher average stacking number of Cat-CCA compared with Cat-Al_2O_3 is attributed to the role of carbon in decreasing the interaction between Al_2O_3 and KCoMoS phase. The observed activity can be explained by 'Rim-Edge' model.[19] According to the model, changing the height/diameter ratio of the crystallite controls the relative quantity of active sites and consequently affects catalytic performance. On the other hand, AC-based catalysts contained a greater proportion of multilayered (CoMoS-II) phase, which is attributed to active phase–support interaction. Thus, increasing the crystallites' linear dimension and stacking degree (*i.e.* increased the edges sites) results in an increase in catalytic activity because this morphologies contain higher ratio of basal, corner and surface sites of the catalyst which are promote HAS. The highest average stacking number and average slab length interpret the highest activity of Cat-BAW. The dispersion results in Figure S12 confirmed the higher agglomeration of BAW and AG-3 that have been characterized by SEM.

In conclusion, microporous support materials based on activated carbon gave higher yields of mainly linear alcohols. Mesopore-dominated support materials showed lower CO conversion and alcohol yields, with a higher proportion of isoalkanols. Most importantly, our study revealed an unexpected relationship between catalytic activity and micro- and mesoporous structures of the supported catalysts. Catalytic activity of catalysts supported on microporous materials was found to be higher than that of catalysts based on mesoporous materials in HAS from syngas. We attributed this phenomenon to distribution of the active phase within the pores and acidity of the catalysts. Catalysts containing large agglomerates of the MoS_2-based active phase supported on microporous materials

exhibited higher activity than catalysts supported on materials with a more mesoporous structure due to the differences in active phase–support interactions. These findings give a deeper insight into the mechanism of HAS over supported transition metal sulfide-based catalysts and catalyst design.

The publication was carried out with the support of the Strategic Academic Leadership Program of the RUDN.

Authors thank Mr. Eugenii Permyakov for fruitful discussion of the results and contribution into responses to the reviewers.

Online Supplementary Materials

Supplementary data associated with this article can be found in the online version at doi: 10.1016/j.mencom.2022.07.026.

References

1 R. Andersson, M. Boutonnet and S. Järås, *Appl. Catal., A*, 2012, 119.
2 M. Ezeldin, V. V. Maximov, V. S. Dorokhov, V. M. Mukhin, T. Sheshko, P. J. Kooyman and V. Kogan, *Catalysts*, 2021, **11**, 1321.
3 S. Zaman and K. J. Smith, *Catal. Rev*., 2012, **54**, 41.
4 R. Andersson, M. Boutonnet and S. Järås, *Fuel*, 2013, **107**, 715.
5 T. D. Dipheko, O. L. Eliseev, Yu. A. Agafonov, M. V. Tsapkina, V. V. Maksimov, M. E. Osman, A. G. Cherednichenko and V. M. Kogan, *Mendeleev Commun*., 2021, **31**, 872.
6 E. A. Permyakov, V. S. Dorokhov, V. V. Maximov, P. A. Nikulshin, A. A. Pimerzin and V. M. Kogan, *Catal. Today*, 2018, **305**, 19.
7 V. V. Maximov, E. A. Permyakov, V. A. Dorokhov, Y. Wang, P. J. Kooyman and V. M. Kogan, *ChemCatChem*, 2020, **12**, 1443.
8 Y. Sakata, Y. Tamaura, H. Imamura and M. Watanabe, *Stud. Surf. Sci. Catal.*, 2006, **162**, 331.
9 M. E. Pérez-Mayoral, V. Calvino-Casilda and E. Soriano, *Catal. Sci. Technol*., 2012, **6**, 1265.
10 Yu. V. Anashkin, D. I. Ishutenko, V. V. Maximov, A. A. Pimerzin, V. M. Kogan and P. A. Nikulshin, *React. Kinet., Mech. Catal.*, 2019, **127**, 301.
11 V. R. Surisetty, A. Tavasoli and A. K. Dalai, *Appl. Catal., A*, 2009, **365**, 243.
12 V. R. Surisetty, A. K. Dalai and J. Kozinski, *Appl. Catal., A*, 2011, **393**, 50.
13 V. R. Surisetty, I. Eswaramoorthi and A. K. Dalai, *Fuel*, 2012, **96**, 77.
14 P. A. Nikulshin, V. A. Salnikov, A. V. Mozhaev, P. P. Minaev, V. M. Kogan and A. A. Pimerzin, *J. Catal*., 2014, **309**, 386.
15 V. S. Dorokhov, M. A. Kamorin, N. N. Rozhdestvenskaya and V. M. Kogan, *C. R. Chim.*, 2016, **19**, 1184.
16 M. Lv, W. Xie, S. Sun, G. Wu, L. Zheng, S. Chu, C. Gao and J. Bao, *Catal. Sci. Technol.*, 2015, **5**, 2925.
17 Y. Liu, K. Murata and M. Inaba, *React. Kinet., Mech. Catal*., 2014, **113**, 187.
18 G. D. Yadav and S. B. Kamble, *Ind. Eng. Chem. Res*., 2009, **48**, 9383.
19 M. Daage and R. R. Chianelli, *J. Catal*., 1994, **149**, 414.

Received: 17th January 2022; Com. 22/6787